用於複合式汽車安定性增强煞車控制器之研究

邱俊智

勤益工商專校機械科

摘　要

本論文主要在描述一個用於複合式汽車（拖曳車和拖車之結合）安定性增强之煞車控制法則。此一控制法則的主要關鍵在於將輪胎力量以輪胎滑動係數和滑動角度之雙線性函數來表示。只要輪胎力量在飽和值以內這種表示是正確的。此一系統即在輪胎側向力量和煞車力量（或加速力量）之間做一協調。更且，當將輪胎力量之雙線性函數帶入汽車數學模式中，此汽車數學模式也會形成一雙線性函數，這是一個重要關鍵，因爲有許多控制方法可用於此種雙線性系統。本論文將根據李雅普諾夫定理推導一安定性增强煞車控制器，再經由電腦模擬以驗證所提出控制器之性能成效。

關鍵詞：煞車控制、雙線性輪胎模型、汽車模型、複合式汽車

STABILITY ENHANCEMENT BRAKING CONTROLLER FOR COMBINATION VEHICLES

Chun-Chih Chiu

Mechanical Engineering Department

Chin-Yi Institute of Technology

ABSTRACT

This paper describes a stability enhancement braking control strategy for combination vehicle(i.e. tow-vehicle and trailer combinations). The key point to develop this controller is a vehicle model in which the tire forces are represented as bilinear functions of wheelslip and slipangle. This tire force representation is valid for tire forces below saturation levels. It captures the essential trade-off between cornering forces and braking (or accelerating) forces. Moreover, when the bilinear equations are substituted into the equations of motion, the resulting vehicle model is bilinear. This is important because a large family of control strategies are available for bilinear systems. These control strategies are based on a Lyapunov Theory. Many forms of controllers can be derived. In this paper a stability enhancement braking controller is derived. Simulation results are presented to demonstrate the performane of the proposed controller.

Key Words: Braking control, Bilinear tire model, Vehicle model, Combination vehicle.

INTRODUCTION

Many papers have been written on the dynamics of combination vehicles (i.e., tow-vehicle/trailer combinations), for example, Jindra (1963) [1], Ellis (1969) [2], and Bundorf (1967) [3]. Papers have also been written on computer simulations of combination vehicle braking systems, for example MacAdam (1985) [4]. But, the emphasis in these papers has been on analysis or simulation accuracy, whereas the emphasis in this paper is on control system development.

Control system development requires simplified models, yet models that retain the essential dynamics of the system to be controlled. In this regard two departures are taken in this paper that distinguish it from previous work. The dynamics equations are vectorized and the tire forces are approximated as bilinear functions of wheelslip and slipangle. The vectorization leads to compact and general equations that apply to many types of vehicle systems and possible controllers. The bilinear approximation leads to tractable equations that still retain the essential trade-off between cornering forces and longitudinal traction forces, namely, that increasing wheelslip decreases cornering force potential and increasing slipangle decreases braking force potential. The vehicle model built from these bilinear equations recognizes this trade-off, and controllers based on it act accordingly. Traditional linear vehicle models can not accomplish this. Moreover, the bilinear equations retain much of the simplicity and tractability of linear equations. They can be manipulated and can be adapt to many real situations.

This paper begins by introducing the bilinear tire model. Plots are given that show the accuracy of the model, and an appendix is provided that discusses model calibration. Then the vehicle equations-of-motion, which are built on the bilinear tire model, are given in their final form. A complete derivation of these is provided in an appendix. These equations turn out to be linear with respect to wheelslip, which is critical in the subsequent derivation of the control strategy. Next, a Lyapunov Function is used to derived a stability constraint that provides a basis for the following control law. Using this constraint the stability enhancement braking controller is derived. Simulation results are provided to demonstrate the effectiveness of the braking controller. The paper ends with conclusions and extensive appendices.

BILINEAR TIRE MODEL

This section introduces the bilinear tire model. It fits tire forces over the region of relatively low slips, beyond those slips where the tire begins to slide. But this is sufficient for control modelling because the controller is designed to keep the tires from sliding. The model is useful because it has the minimum complexity required to capture the trade-off between longitudinal and lateral tire forces. The effectiveness of the model is explored graphically. Appendix A provides more detailed information.

The bilinear tire force equations are (using the subscripts 1 and 2 to designate the longitudinal and lateral tire forces respectively)

$$F_{1i} = \lambda_i(s_{1i} - h_{1i}|\alpha_i|)n_i \quad (1)$$
$$F_{2i} = \alpha_i(s_{2i} - h_{2i}|\lambda_i|)n_i \quad (2)$$

where λ is the wheelslip, α is the slipangle, and n is the normal load. The subscript i refers to wheel i. The s's and h's are coefficients which are chosen to fit the particular tire force data. Methods for selecting these coefficients are given in the appendix.

Notice that for a fixed wheelslip, the longitudinal tire force is diminished by the presence of slipangle, and for a fixed slipangle, the lateral tire force is diminished by the presence of wheelslip. This is the essential trade-off between longitudinal and lateral tire forces. Each equation is linear in one type of slip (either wheelslip or slipangle) while the other is held constant; this is the definition of a bilinear equation. Therefore, these equations can accurately model tire forces over regions of slip where the tire force remains linear in one slip when the other is held constant. This condition holds when the tire is operating at slip levels below those slip levels where the tire begin to "saturate", or "flatten out", and do not increase with increasing slip.

The region of slip levels that produce tire forces below saturation are generally contained within an ellipse, for example

$$\lambda^2 + (\gamma\alpha)^2 < \lambda_0^{*2} \quad (3)$$

where λ_0^* is the wheelslip corresponding to maximum longitudinal tire force (when the slipangle is 0). This region is named the Bilinear Tire-Force Region (BTR). The boundary of this region can be varied according to the specific type of controller being developed. In many cases it can be taken as circular instead of elliptic, by letting γ equal 1, which simplifies the resulting equations.

Notice that if γ is set to 1, then according to Eq. 3, at zero wheelslip, $\alpha^2 < \lambda_0^{*2}$. This implies the slipangle corresponding to the maximum pure cornering force is also equal to λ_0^*. Pure braking forces often saturate at a wheelslip near .15 and pure cornering forces often saturate at a slipangle near .15 radian (8.5 degrees).

The following set of plots illustrates the effectiveness of the bilinear equations. Each plot shows the lateral and longitudinal force as functions of wheelslip and slipangle. There are a series of dotted lines on these plots, and along each dotted line the slipangle is increasing in increments of .01 radian, starting from the right at 0, and working to the left. Along each dotted line the wheelslip is constant. The nonlinear tire data was generated from the model described by Bakker, Nyborg, and Pacejka (1987) [5]. Henceforth this model is referred to as the BNP model.

The first plot, Fig. 1, shows the tire forces generated by varying wheelslip and slipangle over the range from 0 to .2. The second plot, Fig. 2, shows the tire forces generated by varying wheelslip and slipangle over a smaller ranges of slip levels, from 0 to .07 (essentially the BTR). Both of these plots were generated from the BNP model.

Notice that the set of tire forces generated over the larger field of wheelslip and slipangle is not much larger than the set generated over the smaller field. The tire forces at higher slip levels bunch-up and barely extend the set of obtainable forces. Something else happens at

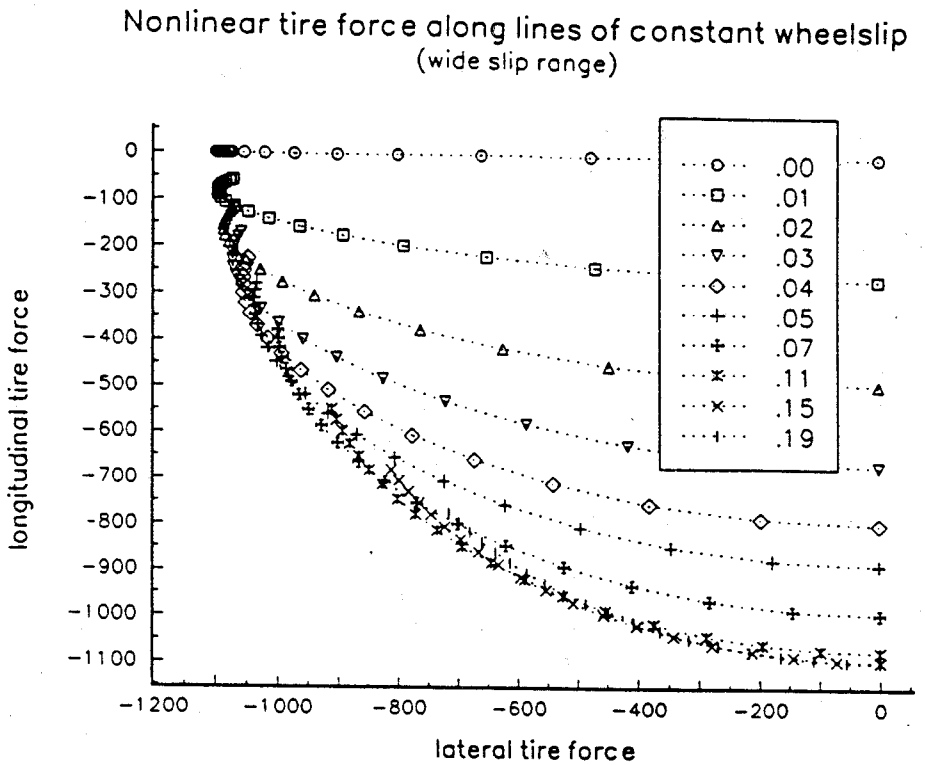

Fig. 1: Nonlinear tire forces over a wide range of slips.

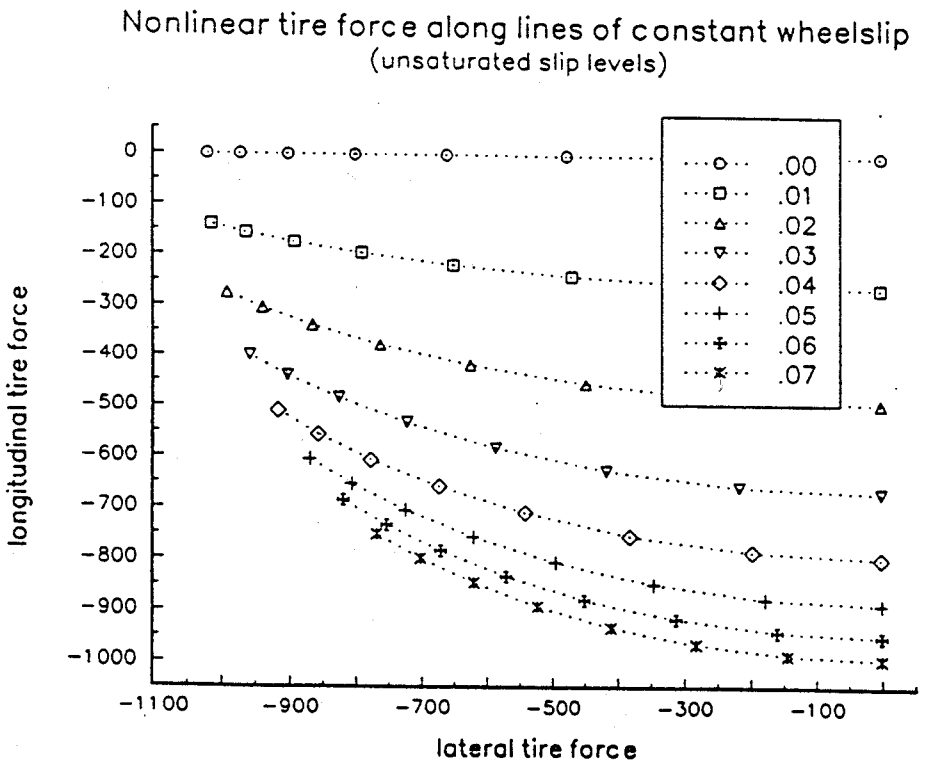

Fig. 2: Nonlinear tire forces over unsaturated slip levels.

high slip levels, namely, the partial derivatives of tire forces with respect to slipangle or wheelslip becomes small. This will cause the vehicle to respond poorly to steering and braking inputs. Based on these observations an important premise can be established. These is little reason to operate at high slip levels, ultimate braking force is not increased by much and directional stability and control are sharply diminished.

A third plot, Fig. 3, shows the tire forces predicted by bilinear equations over the smaller field of slips, the same field as covered in Fig. 2. Notice how well the curves on the bilinear plot match the curves on the nonlinear plot.

A fourth plot, Fig. 4, shows the percent error involved between the bilinear tire model and the nonlinear tire model over the unsaturated region (i.e., the BTR). It is derived by subtracting the predictions of the bilinear model from the values generated from the BNP model and dividing by the values generated by the BNP model. Notice that the percentage error is small at high slip levels and is large at low slip levels.

Emergency brake controllers work at high slip levels, therefore it is appropriate that the bilinear tire model be most accurate at high slip levels for these applications. It is also possible to fit the bilinear tire equations for other regions. For example, it may be desirable to fit the region of low slip levels more closely for a stability enhancement controller that operates at low slip values. Appendix A discusses methods for calibrating the bilinear model by selecting values for the coefficients in Eq.s 1 and 2.

The parameters of the BNP model are determined by trial and error. The particular parameters chosen for the current BNP tire model generate tire forces that are not very linear in wheelslip or slipangle. Even at low slip levels, below saturation, the tire forces follow a convex curve as slip increases. Empirical data indicates that actual tire forces are more linear in wheelslip or slipangle than the current nonlinear model predicts.

EQUATIONS OF MOTION

This section gives the equations of motion of a tow-vehicle/trailer combination in abstract form. These equations are derived in detail in Appendix B.

Using the bilinear tire force equations leads to equations of motion that have the form

$$\dot{u} = f(u,x,d,n,t,p) + U(u,x,d,n,t,p)\lambda \tag{4}$$

and

$$\dot{x} = A(u,n,t,p)x + B(n,t,p)d + D(u,x,d,n,t,p)\lambda + g(u,x,d,n,t,p) \tag{5}$$

where

u- the longitudinal velocity

x- a state vector comprising: v, the tractor side-slip velocity, r, the tractor yaw rate, $\underline{r}$, the trailer yaw rate, and θ, the hitch angle

d- a vector comprising the steering angles of the wheels of the vehicles

n- a vector comprising the normal loads on the wheels of the vehicles

t - a vector comprising the tire properties of the wheels of the vehicles

p- a vector comprising the parameters of the vehicles

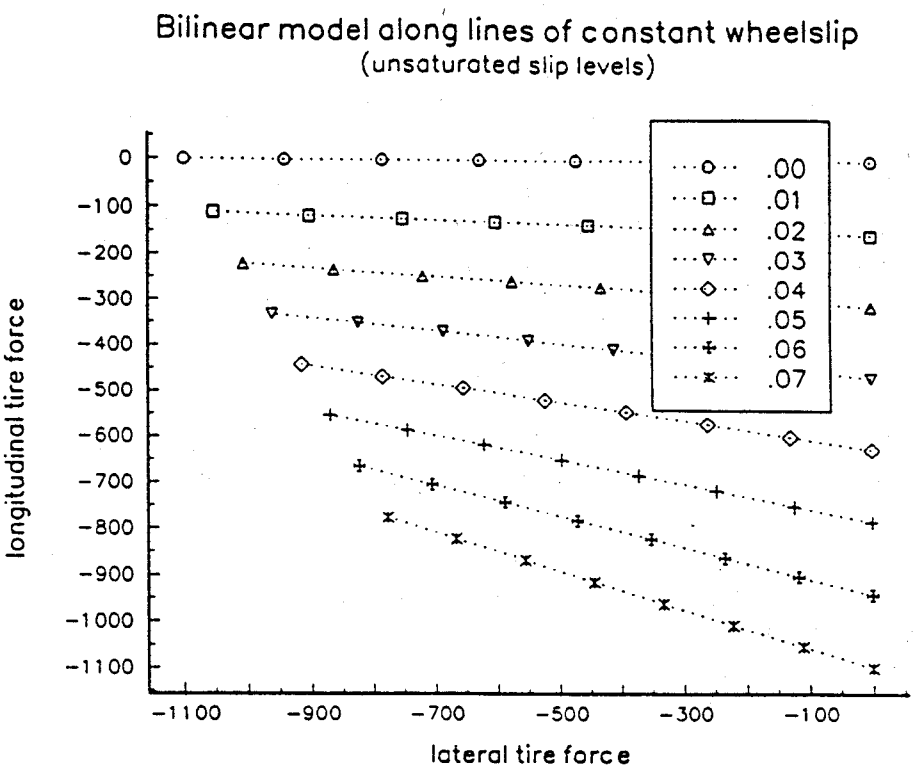

Fig. 3: Bilinear tire force model over unsaturated slip levels.

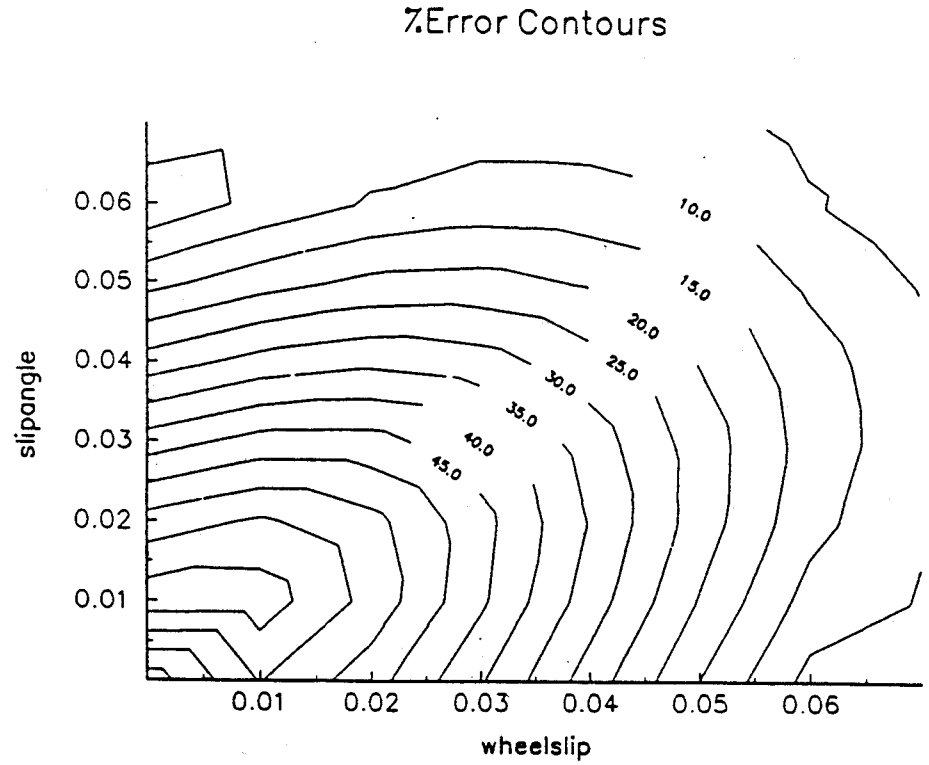

Fig. 4: Error contours for Bilinear tire model.

λ - a vector comprising the wheelslips of the wheels of the vehicles
The matrices A, B, D, and U and the vector functions f and g are defined in Appendix B.

What is important about these equations is that they are linear with respect to λ. This enables application of a class of controllers for Linear-in-Control Systems, see Kalman and Bertram (1960) [6] and Kimbrough (1987) [7]. Another important aspect of these equations is that they are general enough to represent single vehicles or articulated vehicles, and the same approach can be used to design controllers for a broad spectrum of vehicle configurations.

LYAPUNOV STABILITY

The controller described below is based on Lyapunov Theory. It is designed to regulate the ratio-of-reduction of a "disturbance energy" Lyapunov function for the tow-vehicle trailer system. The disturbance energy is defined as the integral (into the future) of the weighted-square of the trajectory errors of the system. Trajectory errors are defined as the difference between the actual stability variables and the states of a reference model. A reference model of the form

$$\dot{x}_{ref} = A_r(u)x_{ref} + B_r d \tag{6}$$

is used to generate a reference trajectory. The A_r and B_r in this equation are typically chosen to closely represent the A and B in Eq. 5. A_r is varied with vehicle speed. The x_{ref} represents the expected trajectory of the vehicle under the conditions that brakes are not applied and there are no external disturbances. Note that formulas for A and B are given in the appendix and these can be used to generate $A_r(u)$ and B_r.

Next, the trajectory error is defined as

$$z = x - x_{ref} \tag{7}$$

One can obtain a Lyapunov function from this of the form

$$z^T p(u) z \tag{8}$$

where P(u) satisfies the Lyapunov Matrix Equation

$$PA_r(u) + A_r^T(u)P = -R\ ; \qquad (R, A_r) \text{ observable} \tag{9}$$

Now it is shown that this Lyapunov function has special significance. Also, it is true that (see Kalman (1960))

$$z^T P(u) z = \int_t^\infty z_r^T(\sigma) R z_r(\sigma) d\sigma \tag{10}$$

where $z_r(\sigma)$ in the trajectory of the system

$$\dot{z}_r(\sigma) = A_r(u(t)) z_r(\sigma) \qquad z_r(t) = z \tag{11}$$

Therefore, the Lyapunov function is the integral from t (meaning the "current time" at which the calculation is made) to the distant future of the weighted square of z_r. And z_r has the initial value of the trajectory error (at the "current time") and evolves according to the reference matrix $A_r(u(t))$ (using the u at the "current time"). Since A_r is always stable the trajectory of z_r decays to zero.

z_r describes the progression of the trajectory error under the conditions that the vehicle model is accurate, that the vehicle does not apply brakes, and that external disturbances do not occur. To see this begin with the definition of z, and using Eq.s 5 and 6

$$\dot{z} = A_r(u)z + (A(u,n,t,p) - A_r(u))x + (B(n,t,p) - B_r)d + D(u,x,d,n,t,p)\lambda + g(u,x,d,n,t,p) \quad (12)$$

and if there is no model mismatch then

$$\dot{z} = A_r(u)z + D(u,x,d,n,t,p)\lambda + g(u,x,d,n,t,p) \quad (13)$$

Furthermore, if the brakes are not applied and there is no model mismatch then the last two terms on the right-hand-side are zero. Hence,

$$\dot{z} = A_r(u)z \quad (14)$$

Comparing this to Eq. 11 reveals that z_r represents the course of the trajectory error, if: 1) the reference model is accurate, 2) there is no wheelslip, 3) there are no external disturbances, and 4) the vehicle speed remains constant. And, if this is true, it follows that the Lyapunov function can be interpreted as the integral of the weighted-square of the trajectory error of the vehicle system.

Obviously these conditions are not true, but this interpretation of z_r is still useful. How so? The reference model can be made accurate to within 20%. The integral is into the infinite future, but it obtains 80% of it value over the first half second. Moreover, the control is recalculated many times a second and constantly resets to the existing vehicle speed.

Therefore a relationship between the Lyapunov function and the trajectory error exists. Although it is approximate it provides a connection between the elements of the weight matrix R and the system performance. The elements of R are the relative weights placed on the elements of z_r. Since z_r approximates the actual trajectory errors, we can think of R as placing weights on the trajectory errors. This is used to direct the priorities of the controller described below.

STABILITY ENHANCEMENT BRAKE CONTROL

The principle of this control law is based on the Lyapunov function just described. The P matrix obtained from Lyapunov Matrix Equation is positive definite and symmetric. Therefore constant value contours of the Lyapunov function z^TPz form ellipsoidal surfaces. A point z represents the current trajectory error. Originating at z is a vector that is perpendicular to the contour; this represents the gradient of the Lyapunov function. The gradient can be found at each point via the formula 2Pz (which is found by simply taking the

gradient of z^TPz). Also originating at z is multiple component vector that constitutes the trajectory of the system, it has the form

$$\dot{z} = A_r(u)z + D(u,x,d,n,t,p)\lambda + m(u,x,d,n,t,p) \tag{15}$$

where

$$m(u,x,d,n,t,p) = (A(u,n,t,p) - A_r(u))x + (B(n,t,p) - B_r)d + g(u,x,d,n,t,p) \tag{16}$$

m contains the nonlinear and model-mismatch terms. Under many conditions vehicles are almost linear, say below .3g. Furthermore, if the reference model A_r and B_r are selected accurately, then the magnitude of m can be small. In any case the magnitude of m can be bounded. This is important, because the bound can be included in the stability constraints described below and this can be used to make the resulting controller "robust".

Our current focus is on the effect that $D(u,x,d,n,t,p)\lambda$ has on the rate-of-reduction of the Lyapunov function. Since the rate-of-reduction along the system trajectory is found by the following equation

$$2z^TP\dot{z} = 2z^TP[A_r(u)z + D(u,x,d,n,t,p)\lambda + m(u,x,d,n,t,p)] \tag{17}$$

then, the effect of applying λ is

$$2z^TPD(u,x,d,n,t,P)\lambda \tag{18}$$

Since λ can be controlled, it is possible to control the effect of this term.

A brake controller is designed to enhance the stability of the vehicle system under conditions where the driver is not demanding hard braking or acceleration. The idea is to use the brakes to help stabilize the vehicle in the event that a significant trajectory disturbance occurs, such as one induced by wind, excessive speed, or other factors. Once disturbed a trailer can begin to swing behind the tow-vehicle and the driver may not be able to dampen the motion. The controller described here applies the system brakes in such a way as to help the combination vehicle recover to its intended trajectory. This idea has been pursued by Presley, Datwyler, and Lorraine (1974) [8], but with the notion of applying both of the trailer brakes simultaneously. The method described here is more effective than this; it operates the brakes independently and with precise timing and is able to obtain greater benefits. It determines at which wheels and when to apply the brakes for the best effect.

The form of the control law follows easily from the basic Lyapunov principle. From examination of Eq. 18 it follows the control law

$$\lambda = -GD^TPz \tag{19}$$

will have a stabilizing effect (i.e., it will increase the rate-of-reduction of the Lyapunov function along system trajectories) if G is a positive semi-definite matrix. To see this, substitute Eq. 19 into Eq. 18 and notice that the effect of the wheelslip becomes

$$-2z^TPDGD^TPz \tag{20}$$

which is negative semi-definite, since G is positive semi-definite. Hence, the use of the wheelslips prescribed by Eq. 19 will accelerate the advance of the vehicle trajectory error to zero.

The generality of G allows for many variations of the control law to be derived. One can select which wheelslips to control or not to control by making G diagonal and placing nonzero gains only on the diagonal elements corresponding to wheel to be controlled. This control law also allows constraints on the elements of λ, for example magnitude constraints such as, $0<\lambda<\lambda_{max}$.

Much insight can be gained by simply examining the control gain matrix, D^TP. The relative magnitudes (when normalized column-wise by the expected ranges of each component of z) of the elements of the matrix D^TP indicate which feedback terms and which wheelslips have the most effect on reducing the rate-of-reduction of the disturbance energy. It is possible to determine the dominant feedback variables and to determine at which wheels the brake control is most effective. These concepts are expored in Kimbrough (1992) [9] for the example case of a pickup truck pulling a utility trailer.

SIMULATION PARAMETERS

This section presents the parameters of a simulation program used to test the effectiveness of the proposed controller. The simulation program considers a combination vehicle consisting of a tractor pulling a semi-trailer. The parameters of the vehicle system are:

tractor mass: 5,600 kg trailer mass: 29,000 kg
tractor width: 2.4 meter trailer wheel base: 10 meter
tractor wheel base: 4.2 meter
distance from tractor c.g. to front axle: .675 meter
distance from tractor c.g. to rear axle: 3.52 meter
distance from trailer c.g. to rear axle: 5 meter
tractor c.g. height: 1.1 meter trailer c.g. height: 2.0 meter
fifth wheel offset: .45 meter fifth wheel height: 1.3 meter
tractor yaw moment of inertia: 12,000 kgm^2
trailer yaw moment of inertia: 277,000 kgm^2
front wheel rotational moment of inertia: 25 kgm^2
tractor rear wheel rotational moment of inertia: 50 kgm^2
trailer rear wheel rotational moment of inertia: 25 kgm^2

The reference model (i.e., A_r and B_r) parameters:
cornering stiffness of tractor: (-153,000 -153,000 -398,000 -398,000) Nt/rad
cornering stiffness of trailer: (-473,666 -473,666) Nt/rad

The simulation model is a yaw plane model. Roll motion and pitch motion are neglected, but load transfer is calculated by quasistatically balancing moments and passing the calculated loads through a low-pass filter with a corner frequency near 2 Hz. The hitch height is considered in the moment calculations. The tractor roll couple distribution is set at 10%

front axle and 90% rear axle. The trailer roll couple distribution is set at 67% fifthwheel and 33% rear axle.

The tire forces are computed via the nonlinear model of Bakker, Nyborg, and Pacejka (1987). The coefficients of the tire model are set the same for all wheels, but the following treatment was employed: The coefficients were chosen for a normal load of 1 kilo-Newton, (kN). The coefficients of the tire model controlling the effects of normal load were selected such that maximum friction was .87 at 1 kN, and this dropped to .75 at 2 kN, and it increased to 1. at .5 kN. Then, when the calculation of tire force was made, the actual normal load was normalized by dividing it by its norminal normal load. The tire forces are then calculated using this number as if it where in kN's. Once the calculation is made for the normalized load it is multiplied by the normal load (in kN's). With this approach the wheels have the same slipangles at low levels of lateral acceleration, but as the lateral acceleration increases, the rear wheels of the tractor (where most the roll couple is resisted) begin to have a greater slipangle than the other wheel sets.

Tire forces do not change instantly with changes in wheelslip or slipangle. They lag. To account for this the simulation program uses tire force filters. The longitudinal tire forces are filtered so that a 90 degree rotation of the wheel is required for them to develop completely. The lateral tire forces are filtered so that a .1 second delay is required for them to develop completely.

The wheel rotational dynamics are modelled. The air-brake system was modelled as a second order system with a corner frequency of 28 radians/second. The transfer function used to relate pressure commands to actual pressures was

$$P_{actual}/P_{command}=1/(s/28+1)^2 \qquad (21)$$

where P_{actual} and $P_{command}$ are the actual and commanded brake pressures. New anti-lock brake systems can achieve this type of response. The commanded brake pressure was determined by a wheelslip regulator, based upon the commanded wheelslip and the measured wheelslip. Many estimators are included in the slip regulator.

The vehicle is tested in open-loop maneuvers without the participation of a driver model. It seems reasonable that a vehicle that is more stable on its own accord will be more stable under driver control, especially if the controller does not introduce higher order dynamics.

SIMULATION RESULTS

The performance of the stability enhancement controller is simulated. The results represent realistic performance expectations because the wheel dynamics and the brake system dynamics are included. Also the estimators required to estimate the feedback variables are simulated. The assumed sensors include: 1) steering wheel position, 2) tractor and trailer yaw rate, 3) wheel speed sensors on each wheel, 4) longitudinal and lateral accelerometers on the tractor, 5) brake pressure sensors, 6) hitch angle sensor.

The combination vehicle begins the simulation with a disturbed initial condition that approximates the mode shape of the swing mode. The initial condition was (.004 m/s, -.024 rad/s, -.022 rad/s, .067 rad) corresponding to tractor side-slip velocity, tractor yaw rate, trailer yaw rate, and the hitch angle. The initial speed is 27.8 m/s (100kph). Only the trailer brakes are applied to enhance stability. Accordingly the G matrix is all zeroes, except for its lower two diagonals which were .05. The weight matrix R is a diagonal matrix with 1, 10, 10, 1 on its diagonal. These weights apply to the tractor side-slip velocity error, the tractor yaw rate error, the trailer yaw rate error, and the hitch angle error respectively. The yaw rate errors are weighted most heavily and the controller places priority on controlling these.

A set of plots convey the results. Fig. 5 shows that the brake stabilized vehicle only slows down about 1 m/s; not a lot of speed is lost. Fig. 6 shows the slip levels employed. Notice the low bandwidth required. This plot also illustrates the action of the wheelslip regulators.

The next two plots show the yaw response and lateral acceleration of the tractor. Fig. 7 shows that the tractor yaw rate is better damped with the stability enhancement controller operating. Fig. 8 shows that the tractor lateral acceleration is also better damped with the satbility enhancement operating. Fig.s 9, 10, and 11 show the trailer yaw rate and lateral acceleration and the hitch angle. These Fig.s also indicate that there is an improvement in damping with the controller operating. This is important because it reduces the likelihood that an accident will occur if the vehicle is disturbed.

CONCLUSIONS

The proposed brake controller shows potential. The simulations indicate that significant improvements are possible. Moreover, these improvements are achievable with existing anti-lock airbrake system; they have adequate response rates. Other requirements are extra sensors and computational hareware. This extra cost may already be justifiable for trucks carrying hazardous cargo. And as the cost of sensors and computers continues to decline the possible applications for these systems will increase.

The stability enhancement controller increases the damping of the vehicle system. It can be installed at minimal cost because, beyond the sensors in an anti-lock brake system, it requires only a hitch angle sensor, a steering wheel sensor, and a trailer yaw rate sensor. Its simplicity arises because it only activates the trailer brakes. This controller was originally developed for passenger vehicles pulling trailers. It was designed to reduce accidents where the trailer begins to swing excessively behind the tow vehicle and knocks it out of control.

Other simulation have been conducted to test this controller, Kimbrough et al. (1990, 1991, 1992) [9, 10, 11, 12]. The results from these simulations show that the steady robust performance can be obtained, in spite of missing and uncertain information and the delays introduced by brake system and tire dynamics. The effects of external disturbances are reduced by over 30% and steerability is improved. The standard test scenario is a lane-change maneuver (under driver model control) on a checkered mu surface, see Kimbrough (1991) [12]. The Linear Program controller completes the maneuver while

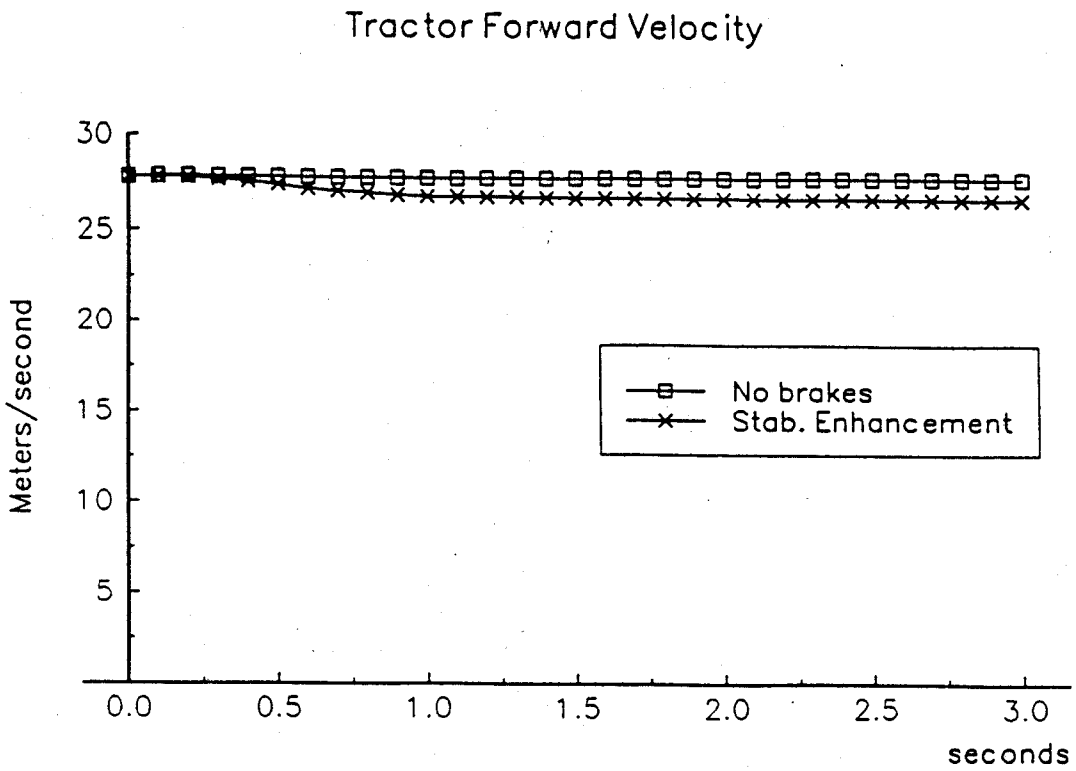

Fig. 5: Tractor speed after disturbance

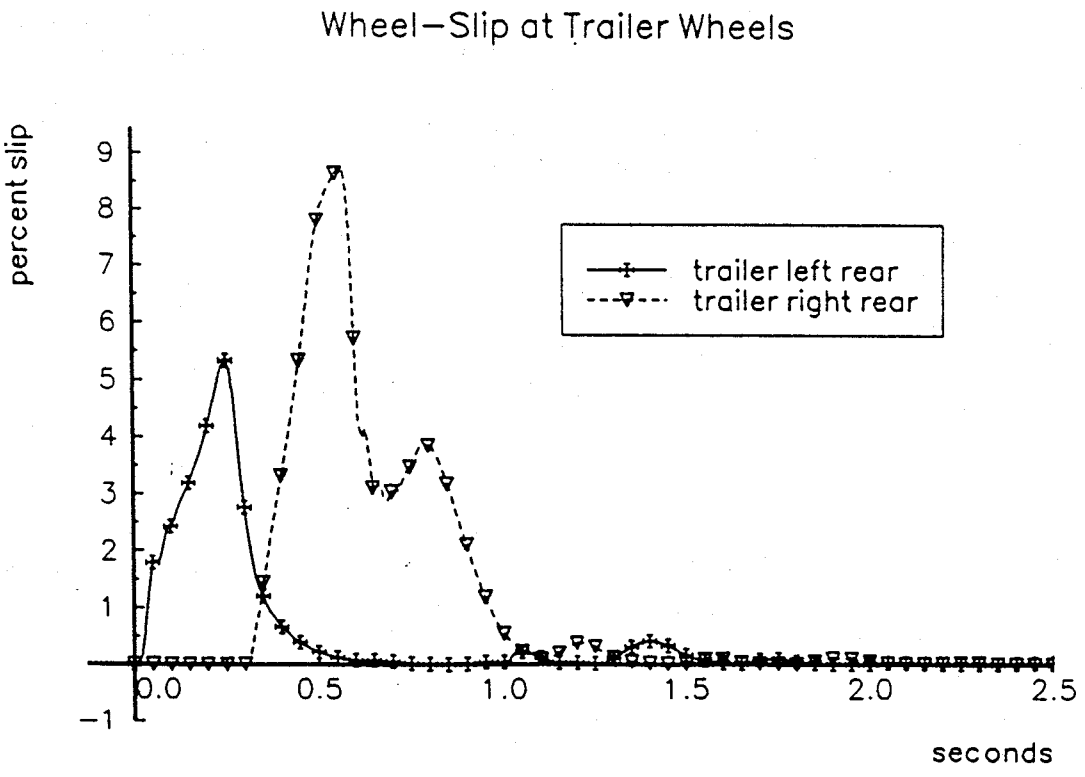

Fig. 6: Wheelslip after disturbance

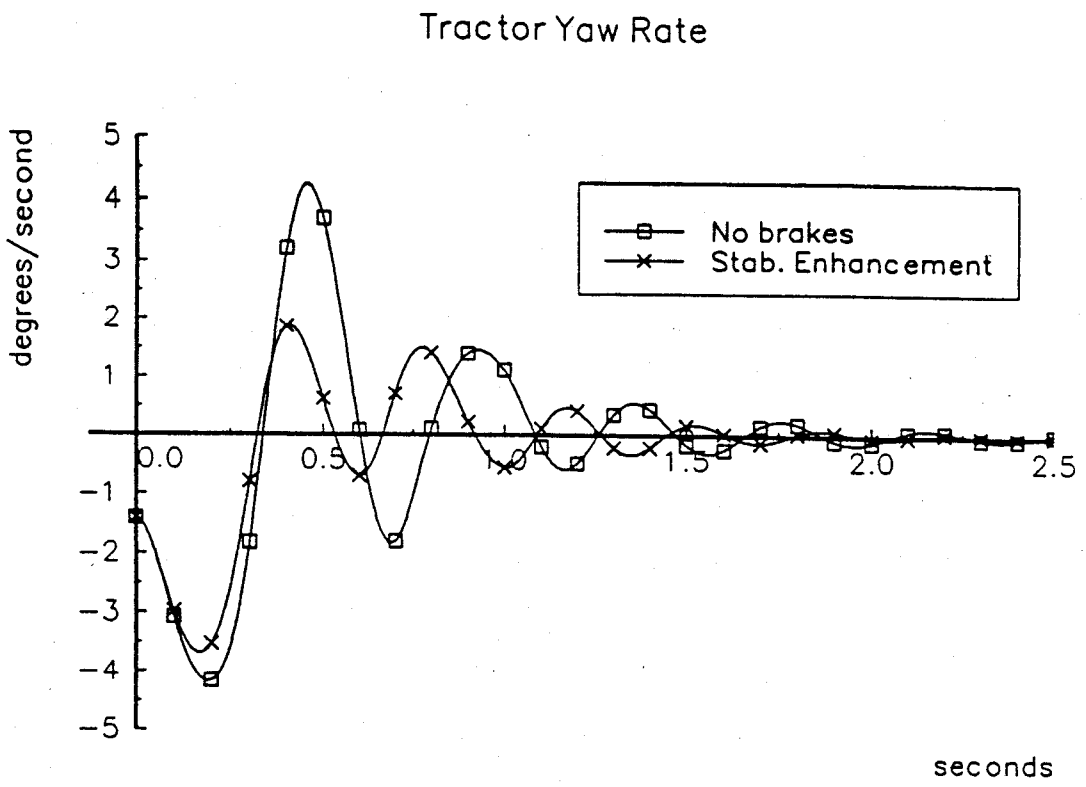

Fig. 7: Tractor yaw rate after disturbance

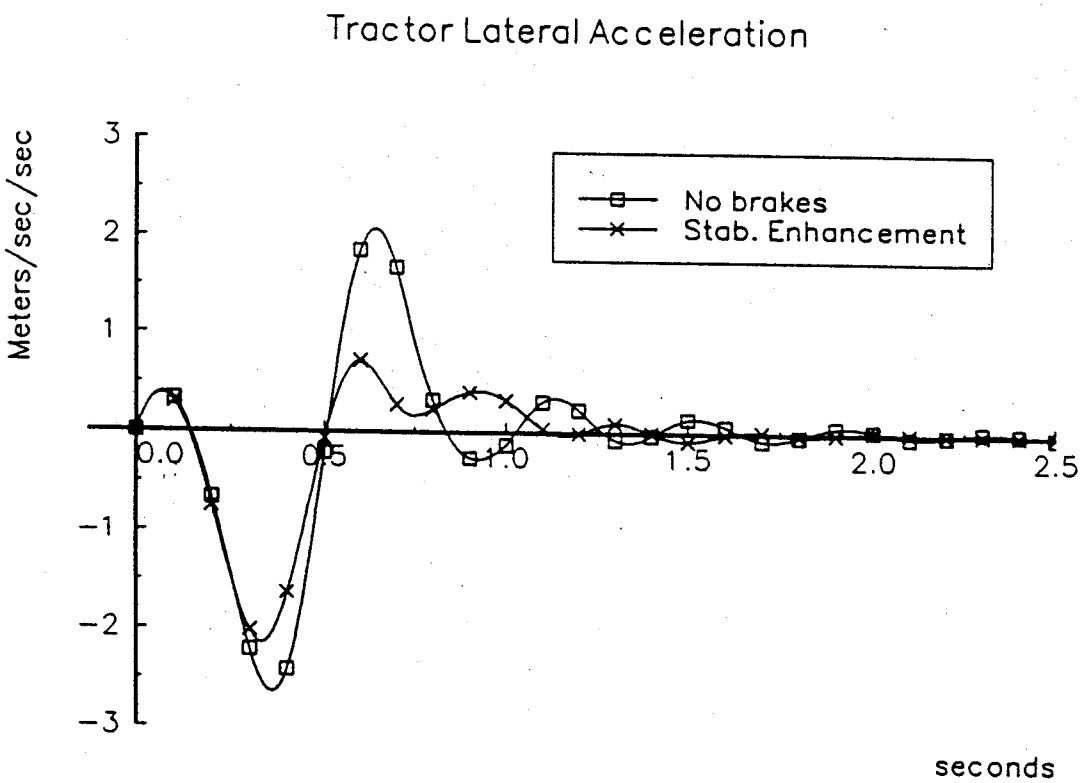

Fig. 8: Tractor lateral acceleration after disturbance

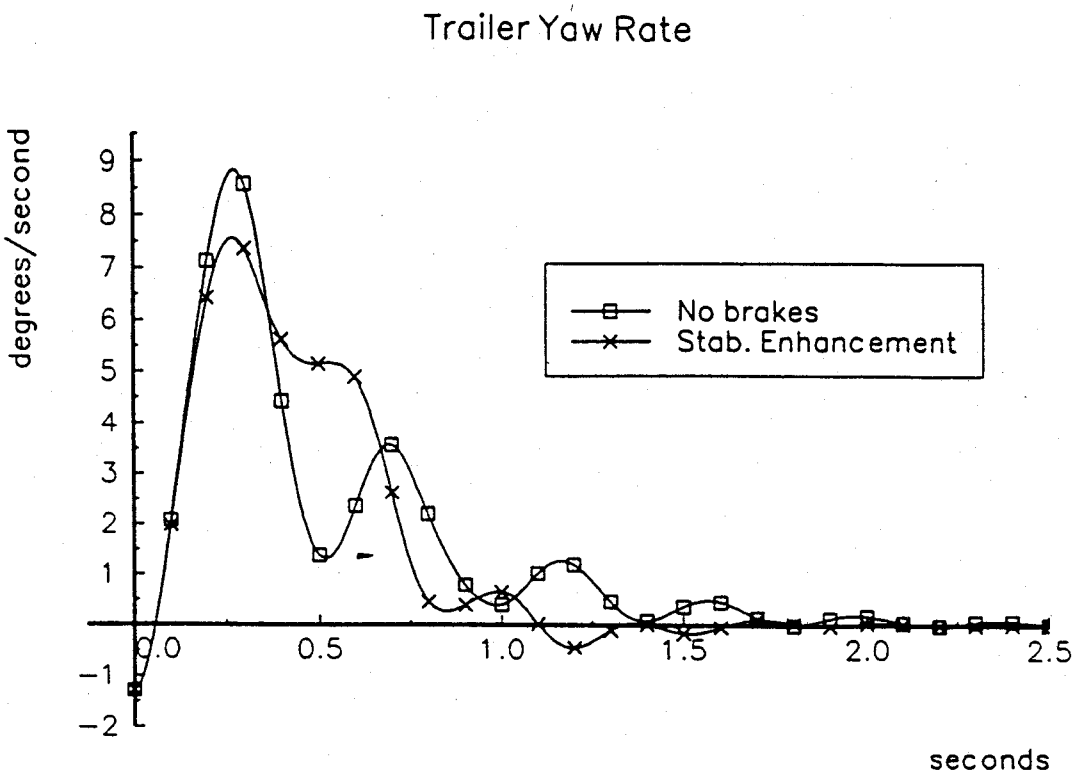

Fig. 9: Trailer yaw rate after disturbance

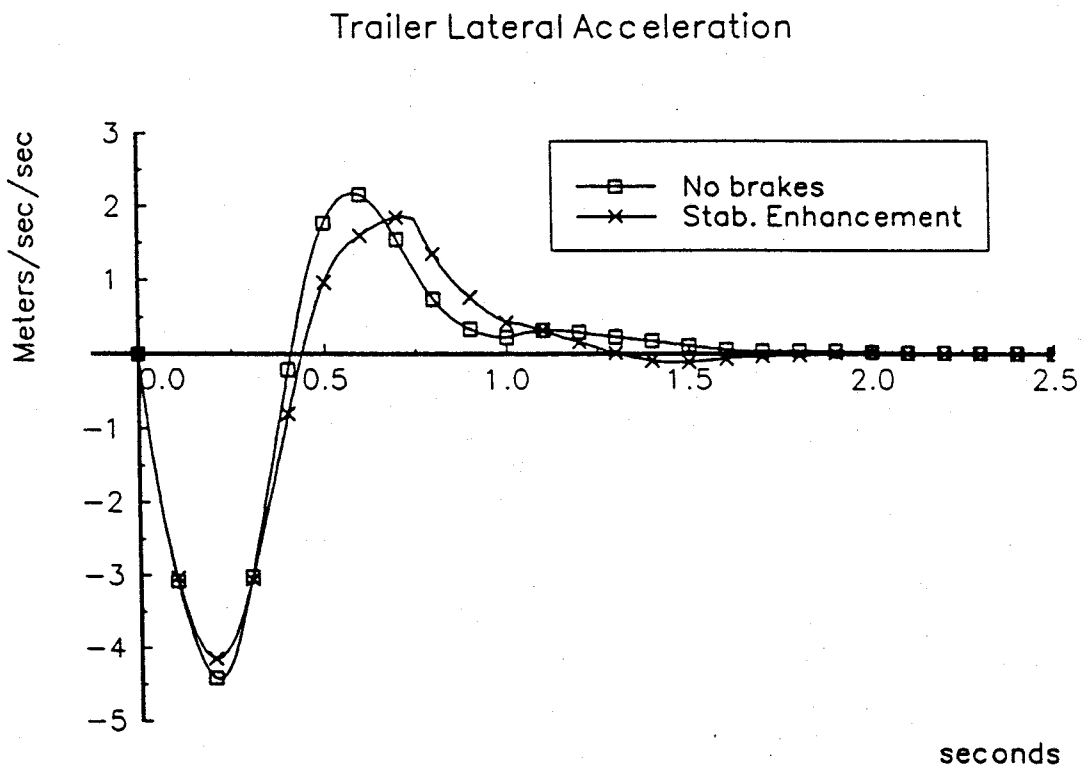

Fig. 10: Trailer lateral acceleration after disturbance

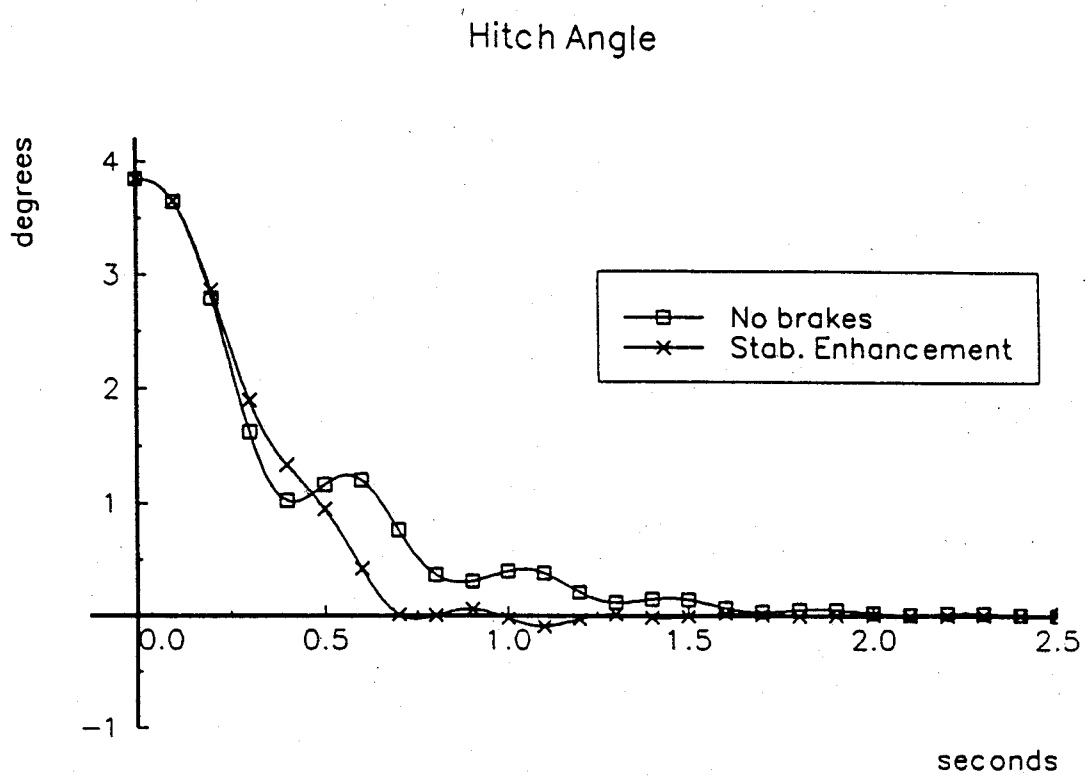

Fig. 11: Hitch angle after disturbance

maintaining stability, whereas other brake strategies, such as peak-seeking and fixed-slip, fail.

REFERENCES

[1] F. Jindra, "Tractor and Semi-Trailer Handing," Automobile Engineer, Oct. 1963

[2] Ellis, J.R., Vehicle Dynamics, London Business Books Ltd., 1969

[3] Bundorf, R.T., "Directional Control Dynamics of Automobile-Travel Trailer Combinations," SAE Transactions, vol. 76, pp. 667-680, 1967

[4] MacAdam, C., "Computer Model Predictions of the Directional Response and Stability of Driver Vehicle Systems During Anti-Skid Braking," Proceedings of the ImechE Conference on Anti-lock Braking Systems for Road Vehicles, U.K., IMechE, 1985

[5] Bakker, E., Nyborg, L., and Pacejka, H., "Tyre Modelling for Use in Vehicle Dynamics Studies," SAE Paper 870421, 1987

[6] Kalman, R.E. and Bertram, J.E., "Control System Design via the Second Method of Lyapunov, Part 1: Continuous Systems," Journal of Basic Engineering, vol. 82, 1960

[7] Kimbrough, S., "Nonlinear Regulators for a Class of Decomposable Systems," ASME J. of DSMC, 1987

[8] Presley, Datwyler, and Lorraine, "Combination Vehicle Yaw Stabilizer," US Patent 3972543, Dec. 6, 1974

[9] Kimbrough, S., and Van Moorhem, W., "Stability Enhancement of Trailers via Selective Actuation of Brakes," ASME 1992 WAM, Transportation Systems, DSC Vol. 44

[10] Kimbrough, S., "Stability Enhancement and Traction Control of Ground Vehicles," Internal Journal of System Science, 1990, Vol. 21, No. 6

[11] Kimbrough, S., and Chiu, C., "Control Strategies for Trailers Equipped with Ateering Systems, ASME 1990 WAM, AMD Vol. 108

[12] Kimbrough, S., and Chiu, C., "A Brake Control Algorithm for Emergency Stops (Which May Involve Steering) of Tow-Vehicle/Trailer Combinations," Proceedings of 1991 American Control Conference

APPENDIX A

This appendix provides details of a bilinear tire model. The basic bilinear tire force equations are

$$F_1 = \lambda(s_1 - h_1|\alpha|)n \quad \text{and} \quad F_2 = \alpha(s_2 - h_2|\lambda|)n$$

where F_1 and F_2 are the braking (accelerating) and cornering tire forces and n is the vertical load on the tires . We also use the convention

$\lambda = 1 - \varpi r_w/u$ for braking
$\lambda = u/\varpi r_w - 1$ for accelerating

where ω is the wheel rotational speed, r_w is the wheel rooling radius, and u is the vehicles longitudinal speed. Since λ is defined as positive for braking it turns out that s_1 and h_1 are negative. We also use the convention

$$\alpha = (v + rl)/u - d$$

where v is the vehicle side-slip velocity, r is the vehicle yaw rate, l is the longitudinal distance from the C.G. to the wheel contact patch, and d is the steering angle of the wheel. With this definition it turns out that s_2 and h_2 are also negative.

This formulation of tire forces is valid for wheelslips and slip-angles below saturation. This region is called the Bilinear Tire-Force Region, (BTR), and as shown above it essentially covers the range of possible tire forces. To simplify developments the BTR will be taken as the interior of a circle whose boundary is

$$\lambda^2 + \alpha^2 = \lambda_0^{*2}$$
or $$\lambda^2 + \alpha^2 = \alpha_0^{*2}$$

where

λ_0^* - the value of wheelslip corresponding to peak longitudinal forcce (when α=0)
α_0^* - the value of slipangle corresponding to peak cornering force (when λ=0)

Ordinarily the BTR is an ellipse but the notation will be simplified if we treat it as a circle. Moreover, for many tires, the BTR is only slightly elliptic. For example, on good roads many tires saturates in wheelslip around λ=.15 and saturate in slipangle around α=.15 radians.

It will turn out to be useful to have certain relationships that can be used to estimate the tire coefficients s and h. The first relationship is

$$s_1 = -\mu_{max}/.8\lambda_0^*$$
$$s_2 = -\mu_{max}/.8\alpha_0^*$$

This comes from the observation that when there is no slipangle then the tire reaches it maximum grip when $\lambda = \lambda_0^*$. The .8 multiplier was used to obtain a better fit to particular tire force data used in this paper. It was required because the slop of the tire force curve was not linear in the "linear region". It exhibited a significant reduction in slop as the slip increased; it was convex down. Without the multiplier the slop was too shallow at low slip levels and it led to under estimates of the forces. When fitting data for more linear tires the .8 multiplier can move towards 1.

To determine the value of h we fit the bilinear equations so that at $\lambda_f = .8\lambda_0^*$ and $\alpha_f = .8\alpha_0^*$, the braking force and cornering force are each only .707 of the magnitude they would have been without simultaneous slip being present, i.e.,

$$\alpha_f(s_2 - h_2|\lambda_f|) = \lambda_f(s_1 - h_1|\alpha_f|) = -.707\mu_{max}$$

which leads to

$$h_1 = h_2 = -.457\mu_{max}/\lambda_0^*\alpha_0^*$$

This calibration technique has worked well in the development of brake controllers, but they may have to be modified as experience is gained with other types of controllers. The use of graphical computer programs is the best way to fine tune the coefficients. After a few hours of experimentation a good understanding of the influences of the coefficients can be developed.

APPENDIX B

This appendix provides the dynamic equations for a tow-vehicle and trailer combination. Fig. B1 illustrates the basic model. Two coordinate systems are used. The first coordinate system is attached to the tow-vehicle center-of-gravity (C.G.). The second coordinate system is attached to the trailer C.G.. A numbering sequence for the wheel of the vehicles is also shown.

The following variables are defined:

u - tractor longitudinal velocity
v - tractor side-slip velocity
r - tractor yaw rate
θ - hitch angle

$\underline{u}$ - longitudinal velocity of trailer
$\underline{v}$ - side-slip velocity of trailer
$\underline{r}$ - trailer yaw rate

The following parameters are defined:

l_i - the longitudinal distance from the tow-vehicle C.G. to its wheel i
t_i - the lateral distance from the tow-vehicle C.G. to its wheel i
h - the longitudinal distance from the tow-vehicle C.G. to the trailer coupling
m - the mass of the tow-vehicle
I - the yaw moment of inertia of the tow-vehicle
$\underline{l}_i$ - the longitudinal distance from the trailer C.G. to its wheel i
$\underline{t}_i$ - the lateral distance from the trailer C.G. to its wheel i
$\underline{h}$ - the longitudinal distance from the trailer C.G. to the trailer coupling
$\underline{m}$ - the mass of the trailer
$\underline{I}$ - the yaw moment of inertia of the trailer

Variables and parameters associated with the trailer are underlined. The values of l_i, t_i, and h (or $\underline{l}_i$, $\underline{t}_i$, and $\underline{h}$) all carry signs. They are positive when directed away from the center-of-gravity in the positive directions of u and v (or $\underline{u}$ and $\underline{v}$).

The following steering angles are defined:

d_i - the steering angle of the tow-vehicle wheels
$\underline{d}_i$ - the steering angle of the trailer wheels

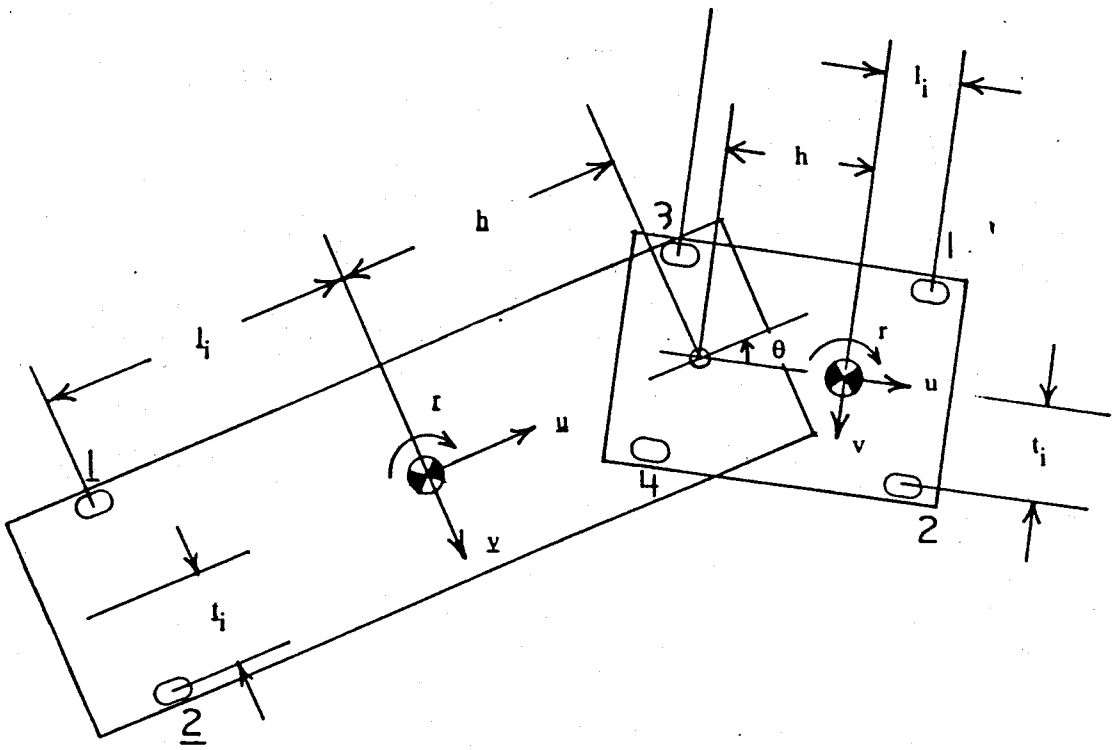

Fig. B.1: Model of tractor/trailer combination that shows states and dimensions.

We also need to define a notation for tire forces.

F_{1i} - the tire force generated along the longitudinal axis of wheel i (the braking or acceleration force)

F_{2i} - the tire force generated perpendicular to the longitudinal axis of wheel i (the cornering force)

The subscripts 1 and 2 are used here because the subscripts x and y refer to the longitudinal and lateral axis of the tow-vehicle.

With the definitions just given, the equations of motion are:

$$\dot{u}(m+\underline{m}) - \dot{r}\underline{mh}\sin\theta = \Sigma F_{1i}\cos d_i - \Sigma F_{2i}\sin d_i - \cos\theta(\Sigma \underline{F}_{2i}\sin \underline{d}_i - \Sigma \underline{F}_{1i}\cos \underline{d}_i) + \sin\theta(\Sigma \underline{F}_{1i}\sin \underline{d}_i + \Sigma \underline{F}_{2i}\cos \underline{d}_i) + (m+\underline{m})vr + \underline{m}hr^2 - \underline{mh}r^2\cos\theta \quad \text{(B1)}$$

$$\dot{v}(m+\underline{m}) + \dot{r}\underline{m}h - \dot{r}\underline{mh}\cos\theta = \Sigma F_{1i}\sin d_i + \Sigma F_{2i}\cos d_i + \sin\theta(\Sigma \underline{F}_{2i}\sin \underline{d}_i - \underline{F}_{1i}\cos \underline{d}_i) + \cos\theta(\Sigma \underline{F}_{1i}\sin \underline{d}_i + \Sigma \underline{F}_{2i}\cos \underline{d}_i) - (m+\underline{m})ur + \underline{mh}r^2\sin\theta \quad \text{(B2)}$$

$$\dot{v}\underline{m}h + \dot{r}(I+\underline{m}h^2) - \dot{r}\underline{mh}h\cos\theta = \Sigma F_{1i}l_i\sin d_i + \Sigma F_{2i}l_i\cos d_i - \Sigma F_{1i}t_i\cos d_i + \Sigma F_{2i}t_i\sin d_i + h\sin\theta(\Sigma \underline{F}_{2i}\sin \underline{d}_i - \Sigma \underline{F}_{1i}\cos \underline{d}_i) + h\cos\theta(\Sigma \underline{F}_{1i}\sin \underline{d}_i + \Sigma \underline{F}_{2i}\cos \underline{d}_i) - \underline{m}hur + \underline{mh}\underline{h}r^2\sin\theta \quad \text{(B3)}$$

$$-\dot{u}(\underline{mh}\sin\theta) - \dot{v}(\underline{mh}\cos\theta) - \dot{r}(\underline{mh}h\cos\theta) + \dot{\underline{r}}(\underline{I}+\underline{h}^2\underline{m}) = -\Sigma \underline{F}_{1i}\underline{t}_i\cos \underline{d}_i + \Sigma \underline{F}_{2i}\underline{t}_i\sin \underline{d}_i + \Sigma \underline{F}_{1i}\underline{l}_i\sin \underline{d}_i + \Sigma \underline{F}_{2i}\underline{l}_i\cos \underline{d}_i - \underline{h}(\Sigma \underline{F}_{1i}\sin \underline{d}_i + \Sigma \underline{F}_{2i}\cos \underline{d}_i) + ru\underline{mh}\cos\theta - \underline{mh}vr\sin\theta - r^2h\underline{hm}\sin\theta \quad \text{(B4)}$$

$$\dot{\theta} = r - \underline{r} \quad \text{(B5)}$$

Eq.s B1-B5 can be expressed in the state-space form as

$$L(\theta)\dot{s} = f(s) \quad \text{(B6)}$$

where L(θ) is an invertible 5 by 5 matrix,

$$L(\theta) = \begin{bmatrix} m+\underline{m} & 0 & 0 & -\underline{mh}\sin\theta & 0 \\ 0 & m+\underline{m} & \underline{m}h & -\underline{mh}\cos\theta & 0 \\ 0 & \underline{m}h & I+\underline{m}h^2 & -\underline{mh}h\cos\theta & 0 \\ -\underline{mh}\sin\theta & -\underline{mh}\cos\theta & -\underline{mh}h\cos\theta & \underline{I}+\underline{mh}^2 & 0 \\ 0 & 0 & 0 & 0 & 1 \end{bmatrix} \quad \text{(B7)}$$

and f(s) is a 5 by 1 vector valued function of the states s, which are (u, v, r, $\underline{r}$, θ).

These equation are now "bilinearized" by substituting in the bilinear tire fore equations.

$$F_{1i} = \lambda_i(s_{1i} - h_{1i}|\alpha_i|) \quad \text{(B8)}$$

$$F_{2i} = \alpha_i(s_{2i} - h_{2i}|\lambda_i|) \quad \text{(B9)}$$

By substitution of these equations into Eq.s B1-B5 we find that

$$L(\theta)\dot{s} = M_1(s)\lambda + M_2(s)\underline{\lambda} + m(s) \tag{B10}$$

where M_1 and M_2 are matrices and m is a vector. What is important here is that the right hand side is linear in λ and $\underline{\lambda}$, the vectors of the wheelslips of the tractor and trailer respectively.

It now becomes desirable to decompose s into u and x, where x is (v, r, $\underline{r}$, θ); u is the longitudinal velocity and x is the remaining states. The system equations are partitioned as

$$L(\theta)\begin{bmatrix} \dot{u} \\ \dot{x} \end{bmatrix} = \begin{bmatrix} U \\ D \end{bmatrix}\lambda + \begin{bmatrix} \underline{U} \\ \underline{D} \end{bmatrix}\underline{\lambda} + \begin{bmatrix} f(s) \\ Ax + Bd + \underline{B}\underline{d} + g(s) \end{bmatrix} \tag{B11}$$

At this point formulas for the components of the matrices are given. The reason for this is because they have the most simple form at this point. Once the left-hand-side matrix is inverted and multiplies by the right-hand-side the terms become much more complex.

In the following formulas the summation signs indicate summation over the number of wheels in the set for the tow-vehicle or in the set for the trailer. Which set is being summed over is indicated by the presence of underlined variables, which implies the trailer; otherwise it is the tow-vehicle. The subscripts (except those on the s's and h's) indicate the row and column of the element being defined.

$$U_{1i} = [(s_{1i} - h_{1i}|\alpha_i|) + \alpha_i h_{2i} d_i]n_i$$
$$\underline{U}_{1i} = [(\underline{s}_{1i} - \underline{h}_{1i}|\underline{\alpha}_i|)(1 + \theta\underline{d}_i) + \underline{\alpha}_i \underline{h}_{2i}(\underline{d}_i - \theta)]\underline{n}_i$$
$$f = -\Sigma \underline{\alpha}_i \underline{s}_{2i}(\underline{d}_i - \theta)\underline{n}_i - \Sigma \alpha_i s_{2i} d_i n_i + (m + \underline{m})vr + \underline{m}(hr^2 - \underline{h}\underline{r}^2)$$
$$D_{1i} = [(s_{1i} - h_{1i}|\alpha_i|)d_i - \alpha_i h_{2i}]n_i$$
$$D_{2i} = [(s_{1i} - h_{1i}|\alpha_i|)(l_i d_i - t_i) - \alpha_i h_{2i}(l_i + t_i d_i)]n_i$$
$$D_{3i} = D_{4i} = 0$$
$$\underline{D}_{1i} = [(\underline{s}_{1i} - \underline{h}_{1i}|\underline{\alpha}_i|)(\underline{d}_i - \theta) - \underline{\alpha}_i \underline{h}_{2i}(1 + \theta\underline{d}_i)]\underline{n}_i$$
$$\underline{D}_{2i} = [(\underline{s}_{1i} - \underline{h}_{1i}|\underline{\alpha}_i|)(\underline{d}_i - \theta) - \underline{\alpha}_i \underline{h}_{2i}(1 + \theta\underline{d}_i)]h\underline{n}_i$$
$$\underline{D}_{3i} = [(\underline{s}_{1i} - \underline{h}_{1i}|\underline{\alpha}_i|)((\underline{l}_i - \underline{h})\underline{d}_i - \underline{t}_i) - \underline{\alpha}_i \underline{h}_{2i}(\underline{l}_i + \underline{t}_i \underline{d}_i - \underline{h})]\underline{n}_i$$
$$\underline{D}_{4i} = 0$$

$$A_{11} = \Sigma s_{2i} n_i / u + \Sigma \underline{s}_{2i} \underline{n}_i / u \qquad A_{12} = \Sigma s_{2i} l_i n_i / u + \Sigma \underline{s}_{2i} h \underline{n}_i / u - (m + \underline{m})u$$
$$A_{21} = \Sigma s_{2i} l_i n_i / u + \Sigma \underline{s}_{2i} h \underline{n}_i / u \qquad A_{22} = \Sigma s_{2i} l_i^2 n_i / u + \Sigma \underline{s}_{2i} h^2 \underline{n}_i / u - \underline{m} h u$$
$$A_{31} = \Sigma \underline{s}_{2i}(\underline{l}_i - \underline{h})\underline{n}_i / u \qquad A_{32} = \Sigma \underline{s}_{2i}(\underline{l}_i - \underline{h})h\underline{n}_i / u + \underline{m}\underline{h}u$$
$$A_{41} = 0 \qquad A_{42} = 1$$
$$A_{13} = \Sigma \underline{s}_{2i}(\underline{l}_i - \underline{h})\underline{n}_i / u \qquad A_{14} = \Sigma \underline{s}_{2i}\underline{n}_i$$
$$A_{23} = \Sigma \underline{s}_{2i}(\underline{l}_i - \underline{h})h\underline{n}_i / u \qquad A_{24} = \Sigma \underline{s}_{2i} h \underline{n}_i$$
$$A_{33} = \Sigma \underline{s}_{2i}(\underline{l}_i - \underline{h})^2 \underline{n}_i / u \qquad A_{34} = \Sigma \underline{s}_{2i}(\underline{l}_i - \underline{h})\underline{n}_i$$
$$A_{43} = -1 \qquad A_{44} = 0$$

$$B_{1i} = -s_{2i} n_i \qquad \underline{B}_{1i} = -\underline{s}_{2i}\underline{n}_i$$
$$B_{2i} = -s_{2i} l_i n_i \qquad \underline{B}_{2i} = -\underline{s}_{2i} h \underline{n}_i$$
$$B_{3i} = 0 \qquad \underline{B}_{3i} = -\underline{s}_{2i}(\underline{l}_i - \underline{h})\underline{n}_i$$

$B_{4i} = 0$ $\qquad\qquad$ $\underline{B}_{4i} = 0$

$g_1 = \Sigma\theta\underline{\alpha}_i\underline{s}_{2i}\underline{d}_i\underline{n}_i + \underline{mhr}^2\theta \qquad g_3 = \Sigma\underline{\alpha}_i\underline{s}_{2i}\underline{t}_i\underline{d}_i\underline{n}_i - \underline{mh}(vr + hr^2)\theta$

$g_2 = (\Sigma\theta\underline{\alpha}_i\underline{s}_{2i}\underline{d}_i\underline{n}_i + \underline{mhr}^2\theta)h + \Sigma\alpha_i s_{2i}t_i d_i n_i \qquad g_4 = 0$

where $\alpha_i = ((v + rl_i)/u) - d_i$ and $\underline{\alpha}_i = ((v + rh + (\underline{l}_i - \underline{h})\underline{r})/u) - \underline{d}_i + \theta$

Having described the elements of the matrices we now continue toward the final form of the equations. Multiplying the equations by the inverse of the left-hand-side matrix yields

$$\dot{s} = L^{-1}M_1\lambda + L^{-1}M_2\underline{\lambda} + L^{-1}m \tag{B12}$$

Once again it is desirable to decompose s into u and x, where x is (v, r, $\underline{r}$, θ). Then, Eq. B7 can be decomposed into the form

$$\dot{u} = U_1\lambda + \underline{U}_2\lambda + f(s) \tag{B13}$$

$$x = D_1\lambda + D_2\underline{\lambda} + Ax + B_1d + \underline{B}_2\underline{d} + g(s) \tag{B14}$$

where Eq. B13 is the top row of Eq. B12, and Eq. B14 is the remaining rows of Eq. B12. In Eq. B14 the terms Ax, B_1d, and $\underline{B}_2\underline{d}$ are the parts of the equations that are linear in x. The term g(s) collects all the nonlinearities. In the equations in the body of the paper λ and $\underline{\lambda}$ are grouped together, so are d and $\underline{d}$. Therefore the U, D, and B in the paper are just U_1 and U_2 together, D_1 and D_2 together, and B_1 and B_2 together, respectively.